
Disulfiram Inhibits Defluorination of ^{18}F -FCWAY, Reduces Bone Radioactivity, and Enhances Visualization of Radioligand Binding to Serotonin 5-HT_{1A} Receptors in Human Brain

Yong Hoon Ryu^{1,2}, Jehi-San Liow¹, Sami Zoghbi¹, Masahiro Fujita¹, Jerry Collins³, Dnyanesh Tipre¹, Janet Sangare¹, Jinsoo Hong¹, Victor W. Pike¹, and Robert B. Innis¹

¹Molecular Imaging Branch, National Institute of Mental Health, National Institutes of Health, Bethesda, Maryland; ²Department of Nuclear Medicine, Yonsei University Medical College, Seoul, South Korea; and ³National Cancer Institute, National Institutes of Health, Bethesda, Maryland

^{18}F -*trans*-4-Fluoro-*N*-2-[4-(2-methoxyphenyl)piperazin-1-yl]ethyl]-*N*-(2-pyridyl)cyclohexanecarboxamide (^{18}F -FCWAY) is a PET radioligand for imaging serotonin 5-hydroxytryptamine-1A receptors in brain. ^{18}F -FCWAY undergoes significant defluorination, with high uptake of radioactivity in the skull and resulting spillover contamination in the underlying neocortex. The cytochrome P450 enzyme CYP2E1 defluorinates many drugs. We previously showed that miconazole, an inhibitor of CYP2E1, blocks defluorination of FCWAY in rats. Here, we used ^{18}F -FCWAY to test the ability of the less toxic agent disulfiram to inhibit defluorination in humans. **Methods:** Eight healthy volunteers underwent a PET scan before and after administration of 500 mg of disulfiram ($n = 6$) or 2,000 mg of cimetidine ($n = 2$). Seven of the subjects had arterial blood sampling during both scans. **Results:** Although cimetidine had relatively small and variable effects on 2 subjects, disulfiram reduced skull radioactivity by about 70% and increased peak brain uptake by about 50% ($n = 5$). Disulfiram decreased plasma-free ^{18}F -fluoride ion (from peak levels of $340\% \pm 62\%$ standardized uptake value (SUV) to $62\% \pm 43\%$ SUV; $P < 0.01$) and increased the concentration of the parent ^{18}F -FCWAY (with a corresponding decrease of clearance from $14.8 \pm 7.8 \text{ L}\cdot\text{h}^{-1}$ at baseline to $7.9 \pm 2.8 \text{ L}\cdot\text{h}^{-1}$ after drug treatment ($P < 0.05$). Using compartmental modeling with input of both ^{18}F -FCWAY and the radiometabolite ^{18}F -FC (*trans*-4-fluorocyclohexanecarboxylic acid), distribution volumes attributed to the parent radioligand unexpectedly decreased about 40%–60% after disulfiram, but the accuracy of the radiometabolite correction is uncertain. Disulfiram changed the shape of the brain time–activity curves in a manner that could occur with inhibition of the efflux transporter P-glycoprotein (P-gp). However, disulfiram showed no in vivo efficacy in monkeys to enhance the uptake of the known P-gp substrate ^{11}C -loperamide, suggesting that the effects of disulfiram in humans were mediated entirely by inhibition of CYP2E1. **Conclusion:** A single oral

dose of disulfiram inhibited about 70% of the defluorination of ^{18}F -FCWAY, increased the plasma concentration of ^{18}F -FCWAY, increased brain uptake of activity, and resulted in better visualization of 5-HT_{1A} receptor in the brain. Disulfiram is a safe and well-tolerated drug that may be useful for other radioligands that undergo defluorination via CYP2E1.

Key Words: metabolism; ^{18}F -FCWAY; 5HT_{1A} receptor; PET; disulfiram; defluorination; serotonin

J Nucl Med 2007; 48:1154–1161
DOI: 10.2967/jnumed.107.039933

The radiometabolites of ^{18}F -*trans*-4-fluoro-*N*-2-[4-(2-methoxyphenyl)piperazin-1-yl]ethyl]-*N*-(2-pyridyl)cyclohexanecarboxamide (^{18}F -FCWAY) in humans and monkeys include an ^{18}F -labeled acid ^{18}F -*trans*-4-fluorocyclohexanecarboxylic acid (FC) and ^{18}F -fluoride ion (*I*). ^{18}F -FC crosses the blood–brain barrier, and PET measurements cannot distinguish the radioactivity of the parent ligand ^{18}F -FCWAY from that of the radiometabolite ^{18}F -FC. This contaminating component of PET brain activity can be mathematically removed by measuring the concentration of ^{18}F -FC in plasma over time and assuming its uptake in humans has the same kinetic parameters as that measured in monkeys (*I*). Another deficiency of ^{18}F -FCWAY is that ^{18}F -fluoride ion adsorbs to bone throughout the body, and radioactivity in skull spills into and artificially increases activity in the underlying neocortex (*2*). The aim of this study was to decrease bone uptake of radioactivity by inhibiting the defluorination of ^{18}F -FCWAY.

The cytochrome P450 isozyme 2E1 (CYP2E1) is a common mediator of drug defluorination in mammals (*3*). The antifungal agent miconazole is a potent inhibitor of CYP2E1 (*4*). We previously showed that miconazole inhibits the defluorination of ^{18}F -FCWAY in rats and markedly reduces bone radioactivity (*5*). In contrast, miconazole

Received Jan. 17, 2007; revision accepted Mar. 16, 2007.
For correspondence contact: Robert Innis, MD, PhD, Molecular Imaging Branch, National Institute of Mental Health, Building 31, Room B2B37, 31 Center Dr., Bethesda, MD 20892-2035.
E-mail: robert.innis@nih.gov
COPYRIGHT © 2007 by the Society of Nuclear Medicine, Inc.

increases brain uptake because of higher concentrations of the parent radioligand in plasma. To decrease defluorination in humans, we selected 2 other CYP2E1 inhibitors: cimetidine and disulfiram. Cimetidine is a relatively weak inhibitor of CYP2E1 inhibitor, with a 50% inhibition constant of more than 3 mM (6). Nevertheless, we selected cimetidine because it can safely be administered at high doses (7). Both disulfiram and its metabolite diethyldithiocarbamate inhibit CYP2E1 in vitro (8). Furthermore, orally administered disulfiram is quite potent, such that a single dose (500 mg), typically used for alcohol abstinence, substantially inhibits defluorination of anesthetic agents in human subjects (9).

The primary goal of this study was to assess the ability of orally administered cimetidine and disulfiram to inhibit defluorination of ^{18}F -FCWAY. We found that disulfiram not only decreased defluorination but also increased brain uptake and delayed the time of peak activity. We wondered whether factors other than metabolic inhibition changed the shape of the brain time–activity curve. Some, but not all, FCWAY analogs that are used as serotonin 5-hydroxytryptamine receptor 1A (5-HT_{1A}) radioligands (10) are substrates for permeability-glycoprotein (P-gp), an efflux pump at the blood–brain barrier. P-gp is located in the endothelium of brain capillaries and prevents the entry of a large range of drugs (11). In addition, metabolites of disulfiram irreversibly inhibit P-gp under in vitro conditions (12). If true in vivo, disulfiram would increase brain uptake of substrates for this transporter. Thus, the secondary goal of this study was to determine whether the effect of disulfiram of increasing brain activity in humans was caused by inhibition of P-gp (i.e., blocking the efflux transporter) as well as CYP2E1 (i.e., inhibiting metabolism and increasing the plasma concentration of parent radioligand). To test whether disulfiram effectively inhibits P-gp in vivo, we used ^{11}C -loperamide, which is an avid substrate for P-gp at the blood–brain barrier (13,14). Loperamide is an opiate agonist used to treat diarrhea and acts via opiate receptors directly on intestinal smooth muscle. Loperamide lacks opiate central nervous system effects, because P-gp prevents its entry into the brain. We tested the ability of disulfiram to increase brain uptake of ^{11}C -loperamide in monkeys and found it was ineffective at doses several times higher than what we used in humans.

MATERIALS AND METHODS

Human Subjects and Drug Administration

Two female and 6 male volunteers (mean age [\pm SD], 28.8 \pm 8.9 y; range, 21–45 y; mean weight, 69.8 \pm 12.3 kg) participated. All subjects were healthy on the basis of history, physical examination, and laboratory testing. The Institutional Review Board of the National Institute of Mental Health approved this study, and all subjects gave written informed consent to participate.

Each subject underwent 2 PET scans, with the first being a baseline scan and the second taking place after drug administration. Six subjects received disulfiram (500 mg orally) about 20 h before the second PET scan. The subjects were told not to drink alcoholic beverages for 1 d before and 14 d after taking disulfiram.

Two different subjects took cimetidine orally before their second PET scan. The subjects took a total of 2,000 mg of cimetidine, with 800 mg taken as a first dose about 16 h before the PET scan and four 300-mg doses taken on the day of the PET scan.

Radiopharmaceutical Preparation

^{18}F -FCWAY was prepared as previously described (15). The injected activity was 298.3 \pm 8.4 MBq, with specific activity of 92.9 \pm 26.8 GBq/ μmol and radiochemical purity greater than 99%.

^{11}C -Loperamide was prepared by treating desmethyl-loperamide (1 mg) with ^{11}C -methyl iodide in dimethyl sulfoxide (400 μL) in the presence of 5 mg of potassium hydroxide (5 mg) at 80°C for 5 min and purifying by high-performance liquid chromatography. Two animals each received 2 injections of ^{11}C -loperamide on the same day. For these 4 preparations, the injected activity was 252 \pm 70 MBq, with specific activity of 63.7 GBq/ μmol and radiochemical purity of 100%.

PET Procedure for Humans

The studies were performed on an Advance tomograph (GE Healthcare), which acquires 35 simultaneous slices with a 4.25-mm interslice distance. Baseline PET scans were acquired in 3-dimensional mode with septa removed, producing a reconstructed resolution of 6–7 mm in all directions. A thermoplastic face mask was used to restrict head movement. After a transmission scan for attenuation correction, 298.3 \pm 8.4 MBq of ^{18}F -FCWAY were administered over 60 s. Emission scans were acquired for 120 min, with frames of 6 \times 30 s, 3 \times 1 min, 2 \times 2 min, and 22 \times 5 min. Up to 40 arterial blood samples were collected to measure radioactivity in whole blood and plasma. In addition, selected samples were used to measure the parent radiotracer ^{18}F -FCWAY and the 2 radiometabolites ^{18}F -FC and ^{18}F -fluoride ion, as previously described (1).

PET Data Analysis

MR images were spatially normalized to the Montreal Neurologic Institute template. The PET images were then spatially normalized and transformed to Montreal Neurologic Institute space through coregistration with the MR images. Skull and gray-matter regions of interest were drawn on multiple contiguous MRI slices of 1 subject. These regions were applied to coregistered PET images of that individual and grouped into 5 anatomic areas: skull; frontal, parietal, and temporal cortices; and cerebellum. The cerebellar volume of interest did not include the vermis, which contains a modest density of 5HT_{1A} receptors (16). Because all PET images were spatially normalized to a common template, the 5 regions of interests were applied directly to other subjects with only minor adjustment. This approach minimized the regional variability that was due to size and shape differences across subjects. Image analysis and compartmental modeling were performed with PMOD 2.75 software (PMOD Technologies Ltd.).

PET activity was expressed as a percentage of the standardized uptake value (SUV), which was normalized for injected activity and body weight and was calculated as (percentage injected activity/ cm^3 tissue) \times (g of body weight).

Activity from the neocortex may have spilled over and artificially increased measurements in the skull. To test this possibility, we imaged 3 bones distant from the brain (cervical vertebrae, mandible, and carpal bones) in a single subject. The carpal bones were chosen because they lack red marrow in adult humans,

unlike the other bones we sampled (skull, cervical vertebrae, and mandible) (17).

Regional radioactivity data were analyzed with a 3-tissue-compartment model: 2 for the parent radioligand ^{18}F -FCWAY (non-displaceable and receptor-bound) and 1 for the brain-penetrating radiometabolite ^{18}F -FC. The model had 2 measured plasma input functions—that is, ^{18}F -FCWAY and ^{18}F -FC. For the radiometabolite ^{18}F -FC, K_1 was fixed at $0.015 \text{ mL}\cdot\text{min}^{-1}\cdot\text{cm}^{-3}$ and V_m at $0.29 \text{ mL}\cdot\text{cm}^{-3}$ for all regions, as previously described (1). These values were determined in monkeys through injection of ^{18}F -FC itself.

Rate constants for the parent radioligand ^{18}F -FCWAY were estimated with weighted least squares and the Marquardt optimizer. Distribution volume is the ratio at equilibrium of brain activity to the concentration of parent radiotracer in plasma (free plus protein-bound). Because we used brain radioactivity, the values represent “total” distribution volume, reflecting both specific and nondisplaceable uptake. Total (V_T) and specific (V_S) distribution volumes were defined according to a recently proposed consensus nomenclature for in vivo imaging of reversibly binding radioligands (18).

$$V_T = \frac{K_1}{k_2} \left(1 + \frac{k_3}{k_4} \right)$$

$$V_S = \frac{K_1 k_3}{k_2 k_4},$$

where K_1 and k_2 are the rate constants of transfer for parent radioligand ^{18}F -FCWAY into and out of the brain, and k_3 and k_4 are the rate constants of association and dissociation, respectively, of the radioligand–receptor complex.

Throughout this article, brain and blood volumes are reported in cubic centimeters and milliliters, respectively, to distinguish the 2 sources of data.

Statistical Analysis

The standard errors of nonlinear least-squares estimation for rate constants were given by the diagonal of the covariance matrix (19) and expressed as a percentage of the rate constants (coefficient of variation [COV]). In addition, the COV of the distribution volume was calculated from the covariance matrix using the generalized form of the error propagation equation (20), where correlations among parameters were considered.

PET Procedure for Animals

We used the Siemens/CTI High Resolution Research Tomograph (Siemens/CPS) to image monkeys with ^{11}C -loperamide and

followed procedures previously described by our laboratory (21). The animals received 500 mg of disulfiram the evening before the scan and a second 500 mg on the morning of the PET scan. The baseline scan of each monkey was acquired on a separate day from the disulfiram scan. The average weight and injected radioactivity for the monkeys were $13.1 \pm 1.8 \text{ kg}$ and $252 \pm 70 \text{ MBq}$, respectively.

RESULTS

Comparison of Disulfiram and Cimetidine

Cimetidine was administered to 2 subjects and, compared with disulfiram, had relatively small and variable effects on the repeated PET scan. For example, skull uptake of radioactivity at 120 min increased by 33% in 1 subject and decreased by 9% in the second. Brain uptake showed similarly variable results. In contrast, disulfiram had dramatic effects that are described in the remainder of the paper.

Both cimetidine and disulfiram were well tolerated, with no subjective adverse effects.

PET of Skull and Other Bones

Under baseline conditions, the skull had high levels of radioactivity by 2 h after injection (Fig. 1A). Coregistered PET and MR images confirmed that this radioactivity derived from the skull. The radioactivity was outside the brain and beneath the subcutaneous fat—related high signal intensity on the T1-weighted MR image (Fig. 1B). Radioactivity in the skull quickly reached 100% of the SUV within 2 min of injection and continued to increase on the baseline scans to about 360% of the SUV at 120 min (Fig. 2A). Although disulfiram had no effect on skull uptake during the initial 2 min, disulfiram blocked all subsequent accumulation during the 2-h scan. The mean percentage SUV of the skull (sampled from the frontal and occipital regions) at 2 h after ^{18}F -FCWAY administration decreased by 67%, from $361\% \pm 88\%$ on the baseline study to $118\% \pm 28\%$ on the study after disulfiram (Figs. 1 and 2A).

The accumulating skull activity above the initial 100% SUV concentration was likely caused by free ^{18}F -fluoride ions, but we are uncertain of the radiochemical identity and even the source of radioactivity during the first 2 min. The injected material had no measurable amounts of free ^{18}F -fluoride ions. Thus, activity from the skull region of interest

FIGURE 1. Horizontal ^{18}F -FCWAY images before and after administration of disulfiram. (A) Baseline image at 2 h shows high activity in skull, consistent with metabolism of ^{18}F -FCWAY to ^{18}F -fluoride ion. (B) Coregistered baseline PET and MR images show skull activity spilling into adjacent brain—for example, into occipital cortex and cerebellum at bottom of image. (C) Repeated PET scan in same subject after disulfiram (500 mg on prior night) shows marked reduction of skull activity and better visualization of brain.

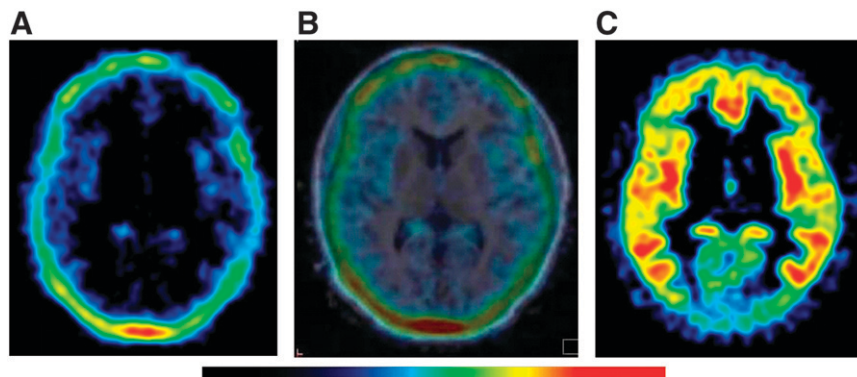


Figure 2

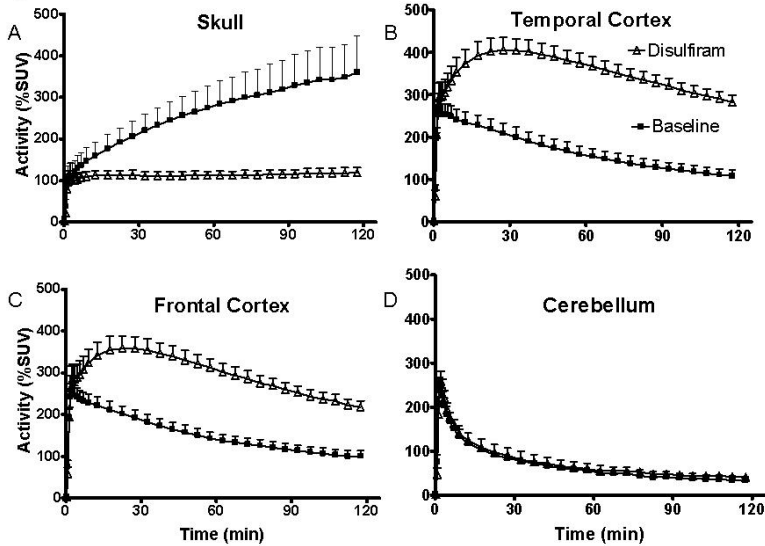


FIGURE 2. Time-activity curves for ^{18}F -FCWAY in brain and skull. (A) Disulfiram had no effect on initial uptake of radioactivity ($\approx 100\%$ SUV) into skull within first few minutes but later blocked continued accumulation seen in baseline conditions. (B and C) In 2 regions (temporal and frontal cortices) with high 5-HT_{1A} receptor densities, disulfiram increased brain uptake and delayed time of peak radioactivity to approximately 30 min. (D) Disulfiram had insignificant effects on time-activity curve in cerebellum, region with few 5-HT_{1A} receptors. Symbols represent mean \pm SD (n = 5).

could represent ^{18}F -FCWAY itself. Alternatively, activity from the skull region of interest may have been derived from the brain because of the limited resolution of the PET camera. In fact, activity in the adjacent neocortex was approximately 275% of the SUV at 2 min, when the skull was about 100% of the SUV. To test this possible partial-volume error, we imaged 1 subject at baseline and after disulfiram to measure activity in 3 bones distant from the brain. Activity was measured at baseline and after disulfiram in the cervical vertebrae, mandible, and carpal bones. We selected carpal bones because they contain no red marrow in adults (17). Disulfiram decreased bone activity at 120 min by 77%, 79%, and 71% in the cervical vertebrae, mandible, and carpal bones, respectively. These values were slightly higher than the mean decline in the skull in 5 subjects (i.e., 67%).

Effect of Disulfiram on Plasma Metabolites

The parent radioligand ^{18}F -FCWAY cleared rapidly from plasma during the baseline study. The concentration of ^{18}F -FCWAY in plasma peaked at about 1 min and decreased to 2.4% \pm 1.2% of that peak by 12 min (Fig. 3). Plasma ^{18}F -FCWAY further decreased at 60 and 120 min to 0.3% \pm 0.1% and 0.2% \pm 0.1% of peak, respectively (Fig. 3). Disulfiram decreased the rapid clearance of ^{18}F -FCWAY. Although the plasma ^{18}F -FCWAY concentration also peaked at about 1 min, disulfiram caused higher plasma concentrations at all subsequent time points. For example, ^{18}F -FCWAY concentrations at 60 and 120 min were 3.4% \pm 0.9% and 2.3% \pm 0.6% of peak, respectively (Fig. 3).

The clearance of ^{18}F -FCWAY was calculated as injected activity divided by area under the curve (AUC) of the ^{18}F -FCWAY plasma concentration extrapolated to infinite time. Disulfiram significantly decreased clearance from 14.8 \pm

7.8 L h⁻¹ at baseline to 7.9 \pm 2.8 L h⁻¹ after drug treatment (P < 0.05 by paired t test).

Disulfiram had no significant effect on the plasma-free fraction (f_p) of ^{18}F -FCWAY, because f_p was 13.3% \pm 1.9% at baseline and 13.6% \pm 3.5% after disulfiram (P = 0.417, by paired t test).

Disulfiram markedly decreased ^{18}F -fluoride ion plasma concentrations (Fig. 4A). Peak levels were 340% \pm 62% of the SUV at baseline and 62% \pm 43% of the SUV after disulfiram (P < 0.01 by paired t test). The plasma ^{18}F -fluoride ion concentration with disulfiram treatment remained relatively stable at about 50% of the SUV from approximately 20 min to the end of the scan (Fig. 4A).

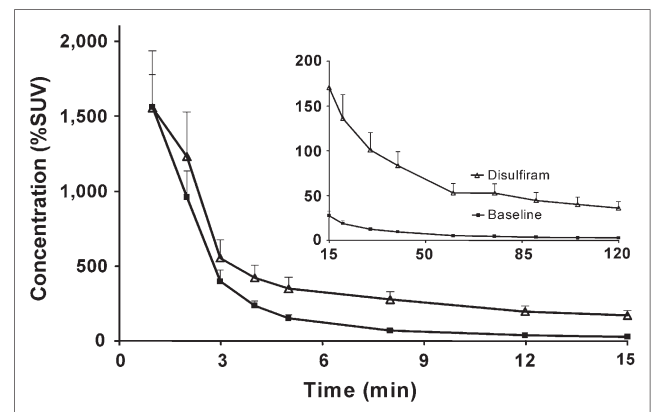


FIGURE 3. Plasma concentration of ^{18}F -FCWAY, separated from radiometabolites. Disulfiram increased concentration of ^{18}F -FCWAY and, thereby, decreased its removal from plasma. Disulfiram significantly decreased clearance of ^{18}F -FCWAY by 47%. Symbols represent mean of 5 subjects, with SD bars only partially visible because some were less than size of symbol itself.

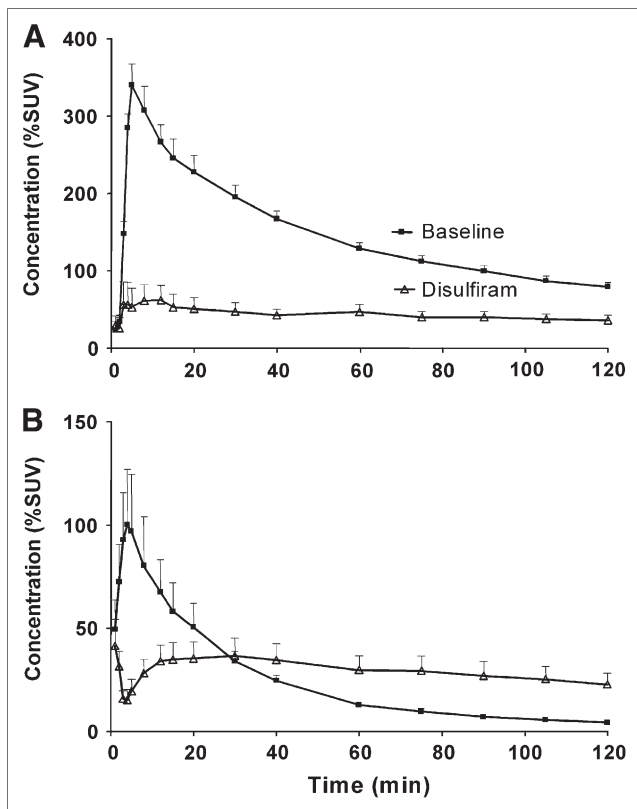


FIGURE 4. Plasma concentration of 2 radiometabolites of ¹⁸F-FCWAY. (A) Disulfiram decreased plasma concentration of ¹⁸F-fluoride ion. Expressed relative to AUC from time 0 to 120 min, disulfiram decreased plasma ¹⁸F-fluoride ion by 69%. (B) Disulfiram had time-dependent effects on plasma concentration of ¹⁸F-FC, initially increasing but later decreasing concentration of this radiometabolite. Symbols represent mean of 5 subjects, with SD bars only partially visible because some were less than size of symbol itself.

Disulfiram had a time-dependent effect on the concentration of ¹⁸F-FC. That is, compared with baseline conditions, disulfiram decreased plasma concentrations of this radiometabolite for the initial 30 min but increased ¹⁸F-FC from 30 to 120 min (Fig. 4B).

Effect of Disulfiram on Brain Radioactivity

On baseline and disulfiram scans, the regional distribution of brain activity was consistent with the densities of 5-HT_{1A} receptors. For example, the highest activities were in the anterior cingulate and medial temporal cortices, and the lowest values were in the cerebellum. From a visual perspective, disulfiram allowed easier identification of the brain, in part by removing the distracting radioactivity from the skull (Fig. 1C). From a quantitative perspective, disulfiram increased brain uptake and delayed the time of peak activity in receptor-rich regions (Figs. 2B and 2C). For example, the approximate peak uptake in the temporal cortex was 400% of the SUV at about 27 min with disulfiram but only 270% of the SUV at about 2 min during baseline (Fig. 2B). In contrast, disulfiram caused no sig-

nificant differences in radioactivity in the 5-HT_{1A} receptor-poor cerebellum (Fig. 2D).

To dissect the various effects of disulfiram on brain time-activity curves, we analyzed PET and plasma data with an unconstrained 2-tissue-compartment model and corrected brain activity for the radiometabolite ¹⁸F-FC. The correction assumes that ¹⁸F-FC has the same K_1 and V_T in humans as that directly measured in monkeys (1). This correction is the method currently used at the National Institutes of Health to analyze human ¹⁸F-FCWAY scans (2,22). Thus, our calculated distribution volumes are supposed to represent specific and nondisplaceable uptake of only the parent radioligand ¹⁸F-FCWAY but would still have variable contamination from skull ¹⁸F-fluoride ion activity.

In the 2-tissue-compartment model, V_T was relatively well identified, with COV values of less than 10% at baseline and after disulfiram (Table 1). However, the individual rate constants k_2 and k_3 (but not K_1 and k_4) showed poor identifiability, with COV values of more than 10% in most regions. Disulfiram decreased the total distribution volume V_T in all regions—for example, by 47% in the frontal cortex and by 71% in the cerebellum (Table 1). To minimize potential changes in nondisplaceable uptake, we also examined the specific distribution volume V_S and found that disulfiram also decreased V_S in all regions (Table 1).

We cannot definitively explain the effects of disulfiram on brain time-activity curves because of its simultaneous effects on skull activity, on the ¹⁸F-FC radiometabolite in plasma, and on clearance of the parent radiotracer ¹⁸F-FCWAY. For example, increased radioactivity in the neocortex after disulfiram was probably caused by higher concentrations of ¹⁸F-FCWAY in the plasma. If so, why did disulfiram cause no change in cerebellar activity? Please note that we did not attempt to strip skull activity from the PET images, because of the questionable accuracy of the method and because we were interested in skull activity itself. Thus, PET measurements of the “cerebellum” were contaminated by spillover from the adjacent skull, and the disulfiram-induced decrease in distribution volumes reflected, in part, decreased bone uptake of ¹⁸F-fluoride ion. To examine a region with negligible bone activity, we also sampled the putamen, which is close to the center of the brain. Nevertheless, disulfiram decreased distribution in the putamen only slightly less than in other regions. Thus, disulfiram effects on distribution volume are not merely due to decreased spillover of activity in adjacent bone.

Effect of Disulfiram on P-gp

A few closely related analogs of FCWAY are substrates for P-gp-mediated efflux from the brain (10, 23). In addition, metabolites of disulfiram are potent *in vitro* inhibitors of P-gp (12). Inhibition of this transporter causes a later peak at a higher value for P-gp substrates, as we found for ¹⁸F-FCWAY after disulfiram in receptor-rich regions of the human brain (Figs. 2B and 2C).

TABLE 1
Mean Distribution Volumes (mL · cm⁻³) at Baseline and After Disulfiram

Site	V _T		V _S		V _S corrected for f _p	
	Baseline	Disulfiram	Baseline	Disulfiram	Baseline	Disulfiram
Frontal cortex						
Distribution volume	7.5 ± 1.1	4.0 ± 15.1	6.9 ± 1.1	3.5 ± 13.4	56.7 ± 9.7	26.2 ± 7.6
COV (%)	3.5 ± 0.4	1.1 ± 0.4	3.7 ± 0.4	1.6 ± 0.6		
Parietal cortex						
Distribution volume	7.3 ± 1.2	4.0 ± 15.5	6.8 ± 1.3	3.5 ± 13.5	56.0 ± 12.7	26.1 ± 7.6
COV (%)	3.3 ± 0.2	1.2 ± 0.4	3.5 ± 0.2	1.6 ± 0.4		
Temporal cortex						
Distribution volume	8.3 ± 1.8	5.1 ± 18.8	7.7 ± 1.8	4.6 ± 16.9	62.9 ± 12.9	33.5 ± 8.6
COV (%)	3.4 ± 0.7	1.2 ± 0.4	3.6 ± 0.7	1.5 ± 0.4		
Cerebellum						
Distribution volume	2.4 ± 1.7	0.7 ± 2.7	1.9 ± 1.6	0.4 ± 1.7	14.6 ± 11.2	2.7 ± 1.6
COV (%)	9.9 ± 9.3	4.7 ± 2.9	14.7 ± 16.9	11.3 ± 7.2		
Putamen						
Distribution volume	2.2 ± 1.3	0.9 ± 3.5	1.8 ± 1.2	0.6 ± 2.4	13.0 ± 7.4	4.5 ± 1.5
COV (%)	10.7 ± 2.4	4.9 ± 1.4	13.3 ± 2.3	7.5 ± 1.3		

To examine whether disulfiram inhibits P-gp *in vivo*, we assessed its effect on brain uptake of ¹¹C-loperamide, which is an avid P-gp substrate (24). Human subjects received 500 mg of disulfiram orally about 20 h before the second PET scan. This dose corresponded to 7.7 mg/kg. We tested 3 monkeys, each of which received two 500-mg doses of disulfiram by mouth. This cumulative dose of 1,000 mg corresponded to 76 mg/kg in these monkeys—that is, almost 10-fold higher than the human dose. Disulfiram caused no significant changes in brain uptake of ¹¹C-loperamide (Fig. 5). As a positive control to ensure that ¹¹C-loperamide is a substrate for P-gp in monkeys, we used tariquidar, which is a potent P-gp inhibitor (25). Tariquidar (8 mg/kg intravenously) was administered 30 min before ¹¹C-loperamide and increased brain activity about 3-fold.

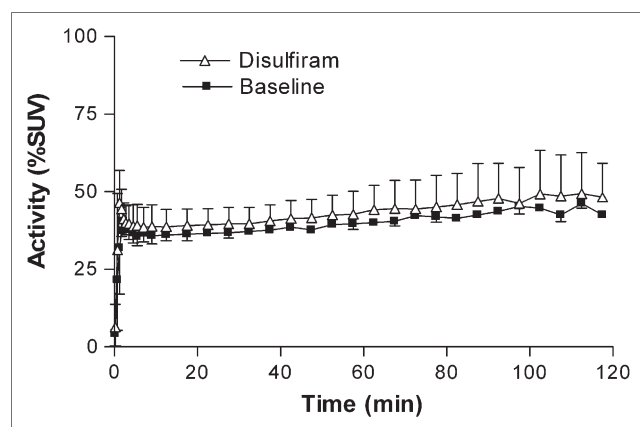


FIGURE 5. ¹¹C-Loperamide brain uptake in rhesus monkeys before and after administration of disulfiram (1,000-mg cumulative dose by mouth). Maximal brain uptake was low (~50% SUV), consistent with loperamide being a substrate for P-gp efflux. Disulfiram had statistically insignificant effects on brain uptake. Symbols represent mean ± SD of 3 animals studied at baseline and after disulfiram.

Thus, ¹¹C-loperamide is a substrate for P-gp in monkeys, and its brain uptake was increased by a known P-inhibitor (tariquidar) but not by disulfiram.

DISCUSSION

Overview

We previously reported that the CYP2E1 inhibitor, miconazole, decreased defluorination, decreased bone uptake of radioactivity, and increased brain activity after injection of ¹⁸F-FCWAY in rats (5). The current study extended this approach to humans. Disulfiram in humans decreased skull radioactivity and increased brain uptake of ¹⁸F-FCWAY. We additionally showed in human plasma that disulfiram decreased the concentration of ¹⁸F-fluoride ion but increased that of the parent radioligand. These results are consistent with the primary mechanism of action of disulfiram: inhibition of the defluorination enzyme CYP2E1. Cimetidine is a weaker CYP2E1 inhibitor than disulfiram and had minimal effects at the doses used in this study. Furthermore, the effects of disulfiram are long-lasting, because it irreversibly inhibits PE21. For example, CYP2E1 activity in humans requires 8 d to return to baseline after a single oral dose of disulfiram (500 mg) (26).

Decreasing the radiodefluorination of PET tracers has several advantages. Tissue measurements are less contaminated by radioactivity from any adjacent bones. The radiation dose to bone marrow will be reduced. The organ itself can be visualized more easily. The concentration of the parent radioligand will tend to be increased and thereby drive more radiotracer into the target tissue. Finally, because more activity goes to the target tissue, the total injected activity can be reduced, thereby reducing the radiation burden to the entire body. We hope this approach can be applied to defluorination of other radioligands. However, several enzymes mediate defluorination, and inhibitors other than disulfiram may be necessary to block their metabolism.

Inhibition of Defluorination

The effectiveness of disulfiram in inhibiting radiodefluorination depends on how the inhibition is calculated. Based on the AUC from 0 to 120 min, disulfiram decreased skull activity (Fig. 2A) by 57%. However, this value likely underestimates the inhibition of defluorination, because the initial "skull" uptake at 2 min included spillover from activity in the adjacent neocortex. More accurate estimates were based on plasma ^{18}F -fluoride ion and PET measurements of radioactivity in bones distant from the brain. Based on the AUC from 0 to 120 min (Fig. 4A), disulfiram decreased plasma ^{18}F -fluoride ions by 69%. We measured bones distant from the brain in 1 subject. Disulfiram decreased bone activity by 71%–79% in the cervical vertebrae, mandible, and carpal bones. Thus, we estimate that disulfiram inhibited about 70% of the defluorination of ^{18}F -FCWAY. The single dose of disulfiram was well tolerated. A repeated dose of 500 mg on the morning of the PET scan, in addition to the 500 mg we administered on the prior evening, may further inhibit defluorination.

Disulfiram had a time-dependent effect on plasma ^{18}F -FC concentrations: increasing before 30 min but decreasing after 30 min. The plasma concentration of any metabolite is the net result of its formation and clearance, including both metabolism and elimination of the metabolite itself. Disulfiram clearly decreased the defluorination of ^{18}F -FCWAY and may have had a similar effect on ^{18}F -FC. Thus, disulfiram would have opposite effects on the concentration of ^{18}F -FC: decreasing its production by inhibiting the metabolism of ^{18}F -FCWAY, and increasing the concentration of ^{18}F -FC by inhibiting its defluorination. The net effect of these 2 actions may have changed during the course of the scan.

Compartmental Analysis

The results of compartmental analysis of the distribution volume must be interpreted cautiously, because disulfiram altered the metabolism of the radioligand and decreased contaminating activity from the skull. From the perspective of clearly interpreting the data, disulfiram fortunately did not alter the plasma free fraction f_p of ^{18}F -FCWAY. If the metabolite correction method for ^{18}F -FC was accurate and if the confounding effects of skull activity were removed, then the distribution volume of the parent radioligand ^{18}F -FCWAY should not change with disulfiram treatment. That is, the higher brain uptake and the later time of the peak after disulfiram should be explained by changes in the input function. In fact, disulfiram blunted the initial rapid decline of plasma ^{18}F -FCWAY before 20 min (which would delay the time of peak brain activity) and increased the plasma AUC (which would increase the AUC of brain activity). The cerebellum region was definitely contaminated by activity from the skull and was not a good region for assessing changes in distribution volume attributed to the parent radioligand ^{18}F -FCWAY. However, regions for the temporal and frontal cortices were drawn at least 1.0 cm

from the skull, and the putamen likely had minimal contamination of bone activity. In fact, disulfiram decreased distribution volumes in the putamen and neocortex similarly to that in the cerebellum (Table 1). We cannot definitively interpret these results, but there are 2 possibilities: Disulfiram may have decreased the density or affinity of 5-HT_{1A} receptors, and the modeling analysis may have been flawed in some way. For example, the metabolite correction for ^{18}F -FC may not apply under both baseline and drug conditions. Inhibition of P-gp by disulfiram is unlikely to have caused the decrease in brain distribution volume. In fact, inhibition of P-gp would increase distribution volume, because brain activity would be increased relative to plasma concentrations.

Possible Effects of P-gp

Because disulfiram was reported to inhibit P-gp (12), we thought this property might explain the delayed peak of ^{18}F -FCWAY brain activity in receptor-rich regions (Figs. 2B and 2C). In addition, we wondered if disulfiram could be used more generally to assess P-gp function in human subjects, because few P-gp inhibitors are available for human use. We gave 2 doses of disulfiram (500 mg) to 3 different monkeys, but it caused insignificant changes in brain uptake of ^{11}C -loperamide, a known substrate for P-gp. As a control experiment, tariquidar (8 mg/kg intravenously), a potent P-gp inhibitor (25), increased brain uptake of ^{11}C -loperamide approximately 3-fold (S. Zoghbi, unpublished data, August 2006). Thus, at least at the doses used (cumulative 1,000 mg), disulfiram showed no blockade of P-gp at the monkey blood–brain barrier. Nevertheless, these experiments were limited, and additional studies are justified.

CONCLUSION

Disulfiram is a potent inhibitor of the liver enzyme CYP2E1, which, among other functions, catalyzes defluorination of several drugs. We found that a single dose of disulfiram (500 mg orally) substantially reduced the defluorination of ^{18}F -FCWAY, as demonstrated by a decreased plasma concentration of the metabolite ^{18}F -fluoride ion and an increased concentration of the parent radioligand ^{18}F -FCWAY. As a consequence, bone activity was markedly reduced and brain activity was enhanced. Because disulfiram has limited toxicity, higher doses may safely provide even greater inhibition and be generally applicable to PET radioligands that undergo radiodefluorination via CYP2E1.

ACKNOWLEDGMENTS

This research was supported by the Intramural Program of the National Institute of Mental Health (project Z01-MH-002795-04). We thank Michel Gottesman, MD, for valuable advice on the function and pharmacology of P-gp; David Sprague and Farris Amanda for subject recruitment and screening; Robert Gladding, CNMT, for technical

assistance; Margaret Der for radiometabolite analysis of plasma samples; Wayne Drevets, MD, and Paul Carlson, MD, for referring subjects; the staff of the NIH PET Department for successful completion of the scanning studies; Xenova Group, Ltd., U.K., for providing tariquidar; and PMOD Technologies, Ltd. (Adliswil, Switzerland), for providing its image analysis and modeling software.

REFERENCES

- Carson RE, Wu Y, Lang L, et al. Brain uptake of the acid metabolites of F-18-labeled WAY 100635 analogs. *J Cereb Blood Flow Metab.* 2003;23:249–260.
- Giovacchini G, Toczek MT, Bonwetsch R, et al. 5-HT_{1A} receptors are reduced in temporal lobe epilepsy after partial-volume correction. *J Nucl Med.* 2005;46:1128–1135.
- Kharasch ED, Thummel KE. Identification of cytochrome P450 2E1 as the predominant enzyme catalyzing human liver microsomal defluorination of sevoflurane, isoflurane, and methoxyflurane. *Anesthesiology.* 1993;79:795–807.
- Tassaneeyakul W, Birkett DJ, Miners JO. Inhibition of human hepatic cytochrome P4502E1 by azole antifungals, CNS-active drugs and non-steroidal anti-inflammatory agents. *Xenobiotica.* 1998;28:293–301.
- Tipre DN, Zoghbi SS, Liow JS, et al. PET imaging of brain 5-HT_{1A} receptors in rat in vivo with ¹⁸F-FCWAY and improvement by successful inhibition of radioligand defluorination with miconazole. *J Nucl Med.* 2006;47:345–353.
- Knodell RG, Browne DG, Gwozdz GP, Brian WR, Guengerich FP. Differential inhibition of individual human liver cytochromes P-450 by cimetidine. *Gastroenterology.* 1991;101:1680–1691.
- Hoogerwerf WA, Pasricha PJ. Pharmacotherapy of gastric acidity, peptic ulcers, and gastroesophageal reflux disease. In: Brunton LL, Lazo JS, Parker KL, eds. *Goodman & Gilman's the Pharmacological Basis of Therapeutics.* 11th ed. New York, NY: McGraw-Hill; 2005:967–982.
- Guengerich FP, Kim DH, Iwasaki M. Role of human cytochrome P-450 IIE1 in the oxidation of many low molecular weight cancer suspects. *Chem Res Toxicol.* 1991;4:168–179.
- Kharasch ED, Thummel KE, Mautz D, Bosse S. Clinical enflurane metabolism by cytochrome P450 2E1. *Clin Pharmacol Ther.* 1994;55:434–440.
- Passchier J, van Waarde A, Doze P, Elsinga PH, Vaalburg W. Influence of P-glycoprotein on brain uptake of [¹⁸F]MPPF in rats. *Eur J Pharmacol.* 2000;407:273–280.
- Ambudkar SV, Dey S, Hrycyna CA, Ramachandra M, Pastan I, Gottesman MM. Biochemical, cellular, and pharmacological aspects of the multidrug transporter. *Annu Rev Pharmacol Toxicol.* 1999;39:361–398.
- Loo TW, Bartlett MC, Clarke DM. Disulfiram metabolites permanently inactivate the human multidrug resistance P-glycoprotein. *Mol Pharm.* 2004;1:426–433.
- Sadeque AJ, Wandel C, He H, Shah S, Wood AJ. Increased drug delivery to the brain by P-glycoprotein inhibition. *Clin Pharmacol Ther.* 2000;68:231–237.
- Passchier J, Lawrie KWM, Bender D, Fellows I, Gee AD. [¹¹C]Loperamide as highly sensitive PET probe for measuring changes in P-glycoprotein functionality [abstract]. *J Labelled Compds Radiopharm.* 2003;46(suppl):S49.
- Lang L, Jagoda E, Schmall B, et al. Development of fluorine-18-labeled 5-HT_{1A} antagonists. *J Med Chem.* 1999;42:1576–1586.
- Parsey RV, Arango V, Olvet DM, Oquendo MA, Van Heertum RL, Mann JJ. Regional heterogeneity of 5-HT_{1A} receptors in human cerebellum as assessed by positron emission tomography. *J Cereb Blood Flow Metab.* 2005;25:785–793.
- Cristy M. Active bone marrow distribution as a function of age in humans. *Phys Med Biol.* 1981;26:389–400.
- Innis RB, Cunningham VJ, Delforge J, et al. Consensus nomenclature for *in vivo* imaging of reversibly binding radioligands. *J Cereb Blood Flow Metab.* In press (doi: 10.1038/sj.jcbfm.9600493).
- Carson R. Parameter estimation in positron emission tomography. In: Phelps M, Mazziotta J, Schelbert H, eds. *Positron Emission Tomography and Autoradiography: Principles and Applications for the Brain and Heart.* New York, NY: Raven Press; 1986:347–390.
- Bevington PR, Robinson DK. Data reduction and error analysis for the physical sciences. New York, NY: McGraw-Hill; 2003:185.
- Yasuno F, Zoghbi SS, McCarron JA, et al. Quantification of serotonin 5-HT_{1A} receptors in monkey brain with [¹¹C](R)-(-)-RWAY. *Synapse.* 2006;60:510–520.
- Bonne O, Bain E, Neumeister A, et al. No change in serotonin type 1A receptor binding in patients with posttraumatic stress disorder. *Am J Psychiatry.* 2005;162:383–385.
- Liow J-S, Lu S, McCarron JA, et al. Effect of P-glycoprotein inhibitor, cyclosporine A, on the disposition in rodent brain and blood of the 5-HT_{1A} receptor radioligand [¹¹C](R)-(-)-RWAY. *Synapse.* 2007;61:96–105.
- Schinkel AH, Wagenaar E, Mol CA, van Deemter L. P-glycoprotein in the blood-brain barrier of mice influences the brain penetration and pharmacological activity of many drugs. *J Clin Invest.* 1996;97:2517–2524.
- Roe M, Folkes A, Ashworth P, et al. Reversal of P-glycoprotein mediated multidrug resistance by novel anthranilamide derivatives. *Bioorg Med Chem Lett.* 1999;9:595–600.
- Emery MG, Jubert C, Thummel KE, Kharasch ED. Duration of cytochrome P-450 2E1 (CYP2E1) inhibition and estimation of functional CYP2E1 enzyme half-life after single-dose disulfiram administration in humans. *J Pharmacol Exp Ther.* 1999;291:213–219.